CHAPTER 4

VALIDATION

The self-consistency and overall quality of the aerosol component measurements are assured by redundancy and intercomparisons between independently measured species. As discussed in Chapter 2, IMPROVE aerosol sampling and aerosol component species measurements proceed in four channels, labelled A through D, with each channel characterized by 1) the type of collection filter used, 2) the measuring technique(s) performed on the collected sample, 3) the species measured, and 4) the particle size range. Validation is a matter of comparing physically or chemically related species that have been measured in different channels. The comparisons discussed in the following sections are the primary ones.

4.1 Sulfur and Sulfate

Sulfur-containing aerosols are measured twice, following the IMPROVE philosophy of redundancy and independent quality assurance for important parameters. Channel A provides a measure of the concentration of elemental sulfur (S), by Proton-Induced X-ray Emission (PIXE) from the aerosol sample collected on a Teflon filter. Channel B provides a measure of the concentration of sulfate ion (SO_4^{2-}), by ion chromatography (IC) of the sample collected on a nylon filter placed behind a gas denuder. The denuder, described in Section 2.1.1, removes gaseous HNO_3 and SO_2 from the sample flow, because they can add artifacts to the particulate nitrate and sulfate measurements. Comparisons of the sulfur and sulfate measurements, presented below, indicate that the Channel A sulfur measurement is not particularly vulnerable to such an SO_2-related artifact. The results of a special study, discussed below and in Appendix B, support this view. Thus, while Channels A and B are independent of each other in both sampling and analysis, the sulfur and sulfate measurements are of the same physical species, ambient particulate sulfate.

The molecular weight of the sulfate ion (96) is three times that of sulfur (32). Therefore, the Channel B measure of sulfate should agree well with 3.0 times the Channel A measure of sulfur. Figure 4.1 shows a typical plot, which indicates generally excellent agreement between these independent measurements. However, the Channel A sulfur measurement is more precise, with a 5% uncertainty, and is therefore used in reconstructions involving the sulfates.

The assumption of no significant artifacts in the above measurements has been questioned. In two studies performed at Canyonlands National Park by Eatough et al. (1991),

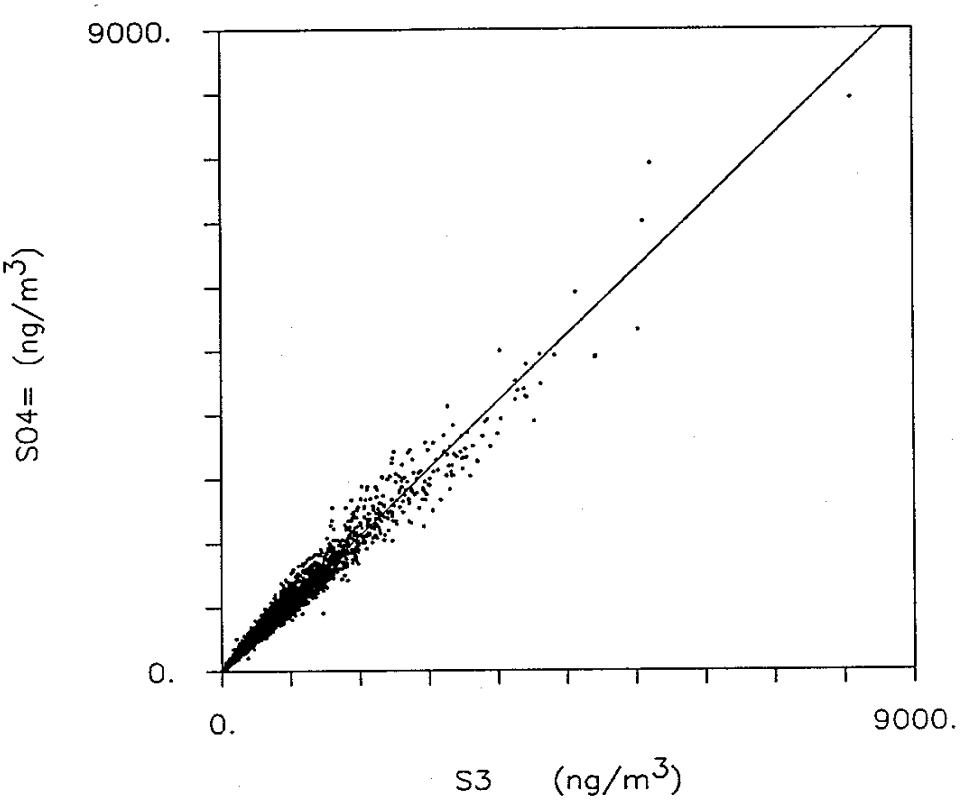

Figure 4.1 Comparison of sulfate on nylon and sulfur (times 3) on Teflon.

a difference in sulfate concentrations of 100 to 300 ng/m^3 was observed between their aerosol sampler modules and ones similar to the IMPROVE modules (but with about five times the flow rate). Eatough hypothesized that SO_2 gas was interacting with alkaline desert fine particles collected on the filter of the IMPROVE type sampler and was being changed to sulfate to produce a significant increase in the measured sulfate concentrations, and a corresponding decrease in the measured SO_2 concentrations. That this artifact was not seen in the samples from their own modules was attributed to their use of a gas diffusion denuder which they believed to be more effective in removing SO_2 than the IMPROVE Channel B denuder.

A comparison study to resolve this issue, involving IMPROVE samplers and samplers constructed by Eatough et al., was performed at Meadview (Lake Mead National Recreational Area, AZ) during the period 20-24 November, 1991. Appendix B is a full report of that study and its results. Table 4.1, excerpted from the report, shows that no SO_2-related artifact was found, regardless of the type of denuder used in sampling. (If there had been such an artifact, measured sulfur concentrations from samples collected without a denuder would have been larger than those from samples collected with a denuder. The "no denuder" samples actually showed slightly smaller sulfur concentrations, on average, than did the samples collected with a denuder, as indicated in Table 4.1 by the negative differences in the last column. However, as reported in Appendix B, these differences are insignificant, being generally below the 5% minimum uncertainty in the

measurement of sulfur by PIXE.) Also, the IMPROVE Channel B denuder was found to remove at least 60% of the SO_2. Thus Channel A must be subject to at least 2.5 times as much artifact as Channel B; however, the comparisons between sulfur and sulfate show no difference. The Meadview study provided overall support and additional validation of IMPROVE aerosol sampling protocols. However, the aerosol conditions during the study were sufficiently in doubt that no final judgement has been made regarding the size of a possible SO_2-related sulfur artifact in IMPROVE. Definitive tests are planned.

Table 4.1 Means and standard errors of sulfur by UCD PIXE in ng/m^3, for samples with and without a denuder. The difference is the "no denuder" value minus the "all denuders" value, and shows the sign of the "artifact".

	Period	Duration	No Denuder	UCD Denuder	EPA Denuder	All Denuders	Difference no - all
1	11/20 AM	6.8h	46±4	47±1	57	50±4	-4±6
2	11/20 PM	13.0h	55±3	59±2	58	59±2	-4±4
3	11/21 AM	9.5h	64±1	68±1	66	67±1	-3±2
4	11/21 PM	13.0h	72±3	74±2	81	76±1	-4±3
5	11/22 AM	9.5h	79±2	80±2	73	78±2	+1±3
6	11/22 PM	13.0h	49±3	48±2	55	50±2	-1±4
7	11/23	30.5h	94±1	90±1	89	89±1	+4±2
8	11/24	24.0h	105±1	106±3	111	108±2	-3±3

4.2 Carbon

Historically, carbon in atmospheric aerosols has been divided into organic and elemental forms, which are currently believed to contribute to light extinction through scattering and absorption, respectively. Elemental carbon is considered the major contributor to light absorption in the atmosphere, with an approximate absorption efficiency of 10 m^2/g. However, analysis of the IMPROVE carbon data, which is also reported in terms of organic and elemental carbon, suggests that significant light-absorbing carbon (LAC) resides in the organic portion. Section 4.2.2 develops this idea.

Carbon in IMPROVE is measured off the Channel C fine quartz filter by the Thermal/Optical Reflectance method (TOR), described in Section 2.1.1. The IMPROVE data provides validation measures for both the organic carbon and the light-absorbing carbon.

4.2.1 Organic Carbon and Hydrogen

Validation of the carbon measurement can be performed by comparing the total organic mass calculated from the Channel C organic carbon (OMC, for Organic Mass by Carbon) with the organic mass calculated from the Channel A hydrogen (OMH). As discussed in Section 3.3.1, OMC and OMH are calculated from:

$$OMC = 1.4(OCLT + OCHT) \tag{4.1}$$

$$OMH = 11(H - 0.250 \cdot S) \tag{4.2}$$

for fully neutralized aerosols. Figure 4.2 shows a plot of OMC vs. OMH for all sites for the first two years of data. The agreement between the two measures of organics is good across all sites. Negative values of OMH are due to acidity at some sites and seasons. Dispersion in the data may be due to uncertainty in the organics measured (see Sec. 2.1.2), as well as acid episodes at some sites or variation in the hydrogen fraction of organics from one site to another.

A major artifact problem associated with the data in the third year, which particularly affected the OMC-OMH comparison in the last year of the data reported on here, is discussed in Section 4.3.

OMC can further be used to investigate the acidity at each site, by studying the variation of H with S and OMC. In the study of acidity, OMC is assumed (on the basis of the comparisons with OMH just presented) to be an appropriate estimate of organic mass, and it is written simply as OM.

Acid aerosols are created by the oxidation of gaseous SO_2 into sulfuric acid (H_2SO_4) under humid conditions. The particulate sulfuric acid scavenges ambient ammonia (NH_3) and is neutralized to the extent that such ammonia is present, to produce either a partially neutralized form such as ammonium bisulfate, $(NH_4)HSO_4$, or fully neutralized ammonium sulfate, $(NH_4)_2SO_4$.

It is assumed that the measured hydrogen is comprised only of portions associated with the sulfates and organics (nitrates and water are volatilized in the vacuum conditions of the hydrogen measurement). Since the sulfates account for all of the measured sulfur, we may write

$$[H] = [H_S] + [H_{OM}] = H_S / S[S] + H_{om} / OM[OM] \tag{4.3}$$

where [H], [S] and [OM] are the concentrations of hydrogen, sulfur and organic matter, respectively; and H_s and H_{om} are the portions of hydrogen associated with sulfur and with organic matter, respectively. The ratio H_s/S depends upon the effective form of the ambient sulfates, and indicates the relative acidity, or neutralization, of the sulfates. H_s/S is 8/32 (0.250) for $(NH_4)_2SO_4$, 5/32 (0.156) for $(NH_4)HSO_4$, and 2/32 (0.063) for H_2SO_4.

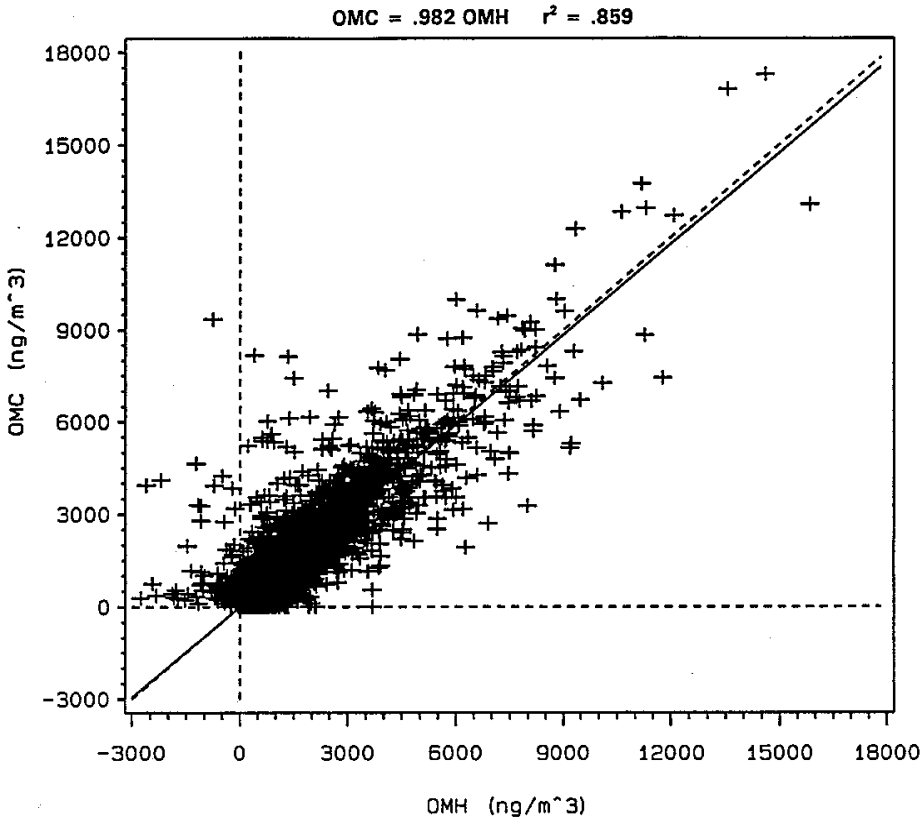

Figure 4.2 Comparison of organic mass on quartz by carbon (OMC) and organic mass on Teflon by hydrogen (OMH).

The H_s/S ratio can be calculated through multivariate regression of H against S and OM over an extended period (generally longer than a single season). Alternatively, if a value for H_{om}/OM is known, H_{om} can be subtracted from H and the value of H_s/S (and hence the acidity) can be studied on a short-term or even individual-sample basis:

$$H_s / S = \left([H] - H_{om} / OM[OM]\right)/[S] \qquad (4.4)$$

A value of $H_{om}/OM=0.09$ was used in the comparisons of OMC versus OMH, and gave very good overall results.

Table 4.2 shows the result of regressions of H against S and OM for every site, taken over the first two years of aerosol data. These regressions indicate an average H_{om}/OM value of 0.067, smaller than the 0.09 value noted above; they also suggest that up to 60% of all sites are "over-neutralized", as indicated by the sulfur regression coefficient (b_1) being greater than the value of 0.250 corresponding to ammonium sulfate. Some sites show up as significantly acidic, including Hawaii Volcanoes in the Pacific; Mount Rainier, Point Reyes, Redwoods and Pinnacles in the Pacific West; Shenandoah in the East; and Tonto in the Sonoran Desert. These sites are expected to be acidic, for the following reasons: 1)The sites near the ocean lack marine sources of ammonia to neutralize the sulfates; 2) Shenandoah is subject to a particularly large sulfate load that requires

more ammonia than may be available for neutralization; and 3) Tonto is near smelters in Southern Arizona and Mexico, and the aerosol may be collected before it has had time to be neutralized. This may also apply to Shenandoah, which is near power plants.

While the regressions generally have good r^2 values, they must be evaluated critically, with consideration of the possible physical and analytical factors that may contribute to these results. For example, the intercept term (b_0) in Table 4.2 arises simply by default in performing an OLS (ordinary least squares) regression, and if the development of Equation 4.1 is correct, this intercept should be zero or nearly so. A significant b_0 term generally means one of several things: 1) that there is a systematic error involved in the measurement of one or more of H, S and OM; 2) that there is a real physical bias involved, such as acidic episodes occurring at higher sulfur loadings; or 3) that there is some other species not accounted for in the derivation of Equation 4.1, such as nitrate in the case of San Gorgonio (where the measured nitrate is about 3 times the measured sulfate, and some may survive the hydrogen measurement), or such as Na_2SO_4 at the coastal and near-coastal sites, where Na^+ ions from sea salt may combine with some of the sulfate ions in solution. Also, and perhaps most importantly, b_0 may be increased by the fact that the uncertainty in measured OM is about five times as large as the uncertainty in measured S. The much greater uncertainty in OM may cause the OLS regression to overestimate both of the coefficients b_0 and b_1 (H_s/S), while underestimating b_2 (H_{om}/OM). (In this regard, the variability in b_2 indicated in the regressions is suspect, particularly those values below 0.06).

The regression method also assumes no correlation between S and OM. Therefore, bias toward higher sulfur coefficients might also arise from the presence of internally-mixed sulfate/organic aerosols causing a significant correlation of S with OM. Also, periods of fires affecting a number of western sites have undoubtedly skewed their data. The regression for Yellowstone was obtained only after the deletion of four outlying observations in organics and hydrogen during the massive fires at that site in the summer of 1988.

Performing variance-weighted regressions should nullify the effect of the excessive uncertainty in OM and substantially reduce the apparent overneutralization. However, even with variance-weighted regressions there is an analytical bias in the data that also has the effect of overestimating the sulfur coefficient. As discussed in Chapter 2, the organics measurement involves a correction for adsorption of organic gases by the collection filter; and this correction appears to have been systematically too large, frequently resulting in negative reported values of organic matter. These negatives have been removed by simply shifting each organics measurement by an amount equal to the largest negative value obtained, for every season of every year at each site. While this correction gives generally reasonable results, it can sometimes fail. This method is tantamount to assuming that the smallest organics measure in a season is zero, if there are negative values reported in the season; also, if no negative values are reported, there is no positive correction at all. In either case, the method allows for an occasional entire season of systematically underestimated organic matter, which can lead to large overestimation of H_s/S. This may be the cause of the high H_s/S value obtained for Denali, for example (see Figure 4.3).

Table 4.2. $H=b_o+b_1S+b_2$ OM regressions.

REGION	SITE	b_o=int	$b_1=H_s/S$	$b_2=H_{om}/OM$	r^2
Alaska	Denali	2±4	.302±.020	.073±.003	.848
Appalachian	Great Smoky Mtns	94±16	.213±.010	.061±.005	.865
	Shenandoah	133±19	.173±.012	.068±.007	.807
Boundary Waters	Isle Royale	41±8	.232±.012	.067±.003	.929
	Voyageurs	26±5	.255±.008	.077±.001	.964
Cascades	Mount Rainier	33±6	.183±.014	.077±.002	.937
Colorado Plateau	Arches	15±5	.273±.017	.074±.004	.854
	Bandalier	39±4	.273±.012	.059±.003	.896
	Bryce Canyon	15±4	.292±.017	.062±.004	.836
	Canyonlands	23±5	.264±.017	.055±.004	.832
	Grand Canyon	11±4	.281±.015	.059±.004	.889
	Mesa Verde	32±4	.319±.013	.026±.003	.823
	Petrified Forest	38±5	.270±.019	.055±.004	.809
Central Rockies	Bridger	11±4	.334±.018	.060±.004	.855
	Great Sand Dunes	27±4	.285±.018	.065±.004	.849
	Rocky Mountains	14±6	.380±.023	.042±.004	.784
	Weminuche	13±5	.349±.019	.053±.004	.834
	Yellowstone	25±6	.229±.023	.074±.003	.823
Pacific Coastal	Pinnacles	13±9	.186±.019	.088±.003	.853
	Point Reyes	3±9	.155±.020	.099±.003	.890
	Redwoods	33±5	.148±.016	.068±.002	.888
Florida	Everglades	-13±13	.231±.017	.082±.003	.903
Great Basin	Jarbidge	25±4	.372±.032	.051±.004	.782
Hawaii	Hawaii Volcanoes	24±5	.186±.004	.038±.013	.916
Northeast	Acadia	34±8	.236±.009	.067±.004	.930

Table 4.2 Continued

REGION	SITE	b_o=int	b_1=H_s/S	b_2=H_{om}/OM	r^2
Northern Great	Badlands	27±5	.247±.012	.068±.003	.890
Northern	Glacier	42±7	.231±.025	.066±.002	.893
Southern California	San Gorgonio	30±17	.298±.068	.096±.010	.791
Sonoran Desert	Chiricahua	16±5	.296±.011	.068±.004	.912
	Tonto	-55±24	.157±.051	.168±.010	.668
Sierra	Yosemite	17±5	.312±.018	.071±.002	.932
Sierra	Crater Lake	15±6	.443±.045	.048±.004	.786
	Lassen Volcanoes	23±4	.303±.028	.062±.003	.851
Washington DC	Washington	8±10	.291±.012	.074±.007	.953
West Texas	Big Bend	32±6	.257±.011	.056±.004	.896
	Guadalupe Mtns	38±7	.309±.012	.029±.005	.835

At the heart of the regression method is the fact that, aside from analytical or measurement biases and the possibility of unaccounted species at some sites, the quality of the long-term regression depends upon there being an actual value of H_s/S (and of H_{om}/OM) about which the ratio varies randomly and by only a limited amount, for all samples during the period of the regression. This means that the sulfate should have about the same average form (and the organics should have about the same average fraction of hydrogen) throughout. This should be the case at sites with periods during which the sulfates are fully neutralized, for example; and, while H_s/S would change during acid episodes, H_{om}/OM may be stable in such epsodes. Cases of a nearly constant value of H_s/S could allow an accurate determination of H_{om}/*OM*, according to:

$$H_{om} / Om = ([H] - H_s / S[S]) / [OM] \qquad (4.5)$$

From this value of H_{om}/OM, changes in H_s/S that occur in other periods might be followed.

In general, there are a number of uncertainties involved in the calculation of acidity, whose separate effects are not easily discriminated. More detailed studies are being performed, however, and the method discussed herein may hold some promise both as a measure of aerosol acidity and a check on the ambient organic forms in aerosols.

4.2.2 Elemental Carbon and Light Absorption

The carbon measurements can also be compared with the light absorption measurement, b_{abs}. Based on the previous discussion of light-absorbing and organic carbon, b_{abs} should correlate well with elemental carbon, but not with OCLT or OCHT (unless the elemental and organic carbons are well correlated with each other). However, this is not the case.

Figures 4.4a and 4.4b show scatter plots of b_{abs} vs. each of the four carbons at selected sites. (Scatter plots for all of the sites are presented in Appendix C.) It can be seen that ECHT often shows little or no correlation with b_{abs}, except at sites (particularly in the West) where the amount of ECHT is comparable to the ECLT; and even then, ECLT and ECHT show little correlation with one another. Instead, surprisingly, b_{abs} is well correlated with both ECLT and OCHT. (There is sometimes even an indication of correlation between b_{abs} and OCLT). These results suggest the possibility that light-absorbing carbon may be primarily divided between OCHT and ECLT.

At many sites, OCHT and ECLT are well correlated, and it might be supposed that the correlation of b_{abs} with OCHT could be entirely explained as due to the ECLT associated with the OCHT, and not because OCHT itself absorbs light. However, if ECLT is responsible for most of the light absorption, then theory would suggest that the ratio b_{abs}/ECLT--the absorption efficiency of the ECLT--should be between about 8 and 12 m^2/g. However, many sites have ratios of b_{abs}/ECLT that are twice the expected value. This suggests that OCHT could contribute approximately half of the light absorption.

Furthermore, at other sites, particularly in a number of the western regions, there is a good deal more scatter between OCHT and ECLT, yet it is OCHT that correlates better with b_{abs} than does ECLT (Figure 4.4b). Also, the scatter plots of b_{abs} vs. ECLT at these sites (which show a limiting, minimum b_{abs}/ECLT ratio of about 20 m^2/g, with dispersion above that line) are quite similar to the corresponding scatter plots of OCHT vs ECLT (which also show a limiting, minimum OCHT/ECLT ratio, of about 3 or 4, with dispersion above that line). These plots do not rule out the possibility that other absorbing species exist which happen to correlate with OCHT. However, they suggest that b_{abs} fails to correlate with ECLT precisely to the extent and in the same manner that OCHT does not correlate with ECLT, and therefore, that OCHT contains much or most of the light-absorbing carbon not accounted for by ECLT.

In fact, the scatter plots, and hence the correlations, of both ECLT and ECHT with b_{abs} tend to mimic the forms of their respective scatter plots with OCHT. Thus, for example, what little correlation is shown at some sites between b_{abs} and ECHT appears to depend upon the corresponding correlation between OCHT and ECHT at those sites. The conclusion is that even at sites where ECHT is comparable to ECLT, OCHT may contain approximately as much light-absorbing carbon as do ECLT and ECHT put together.

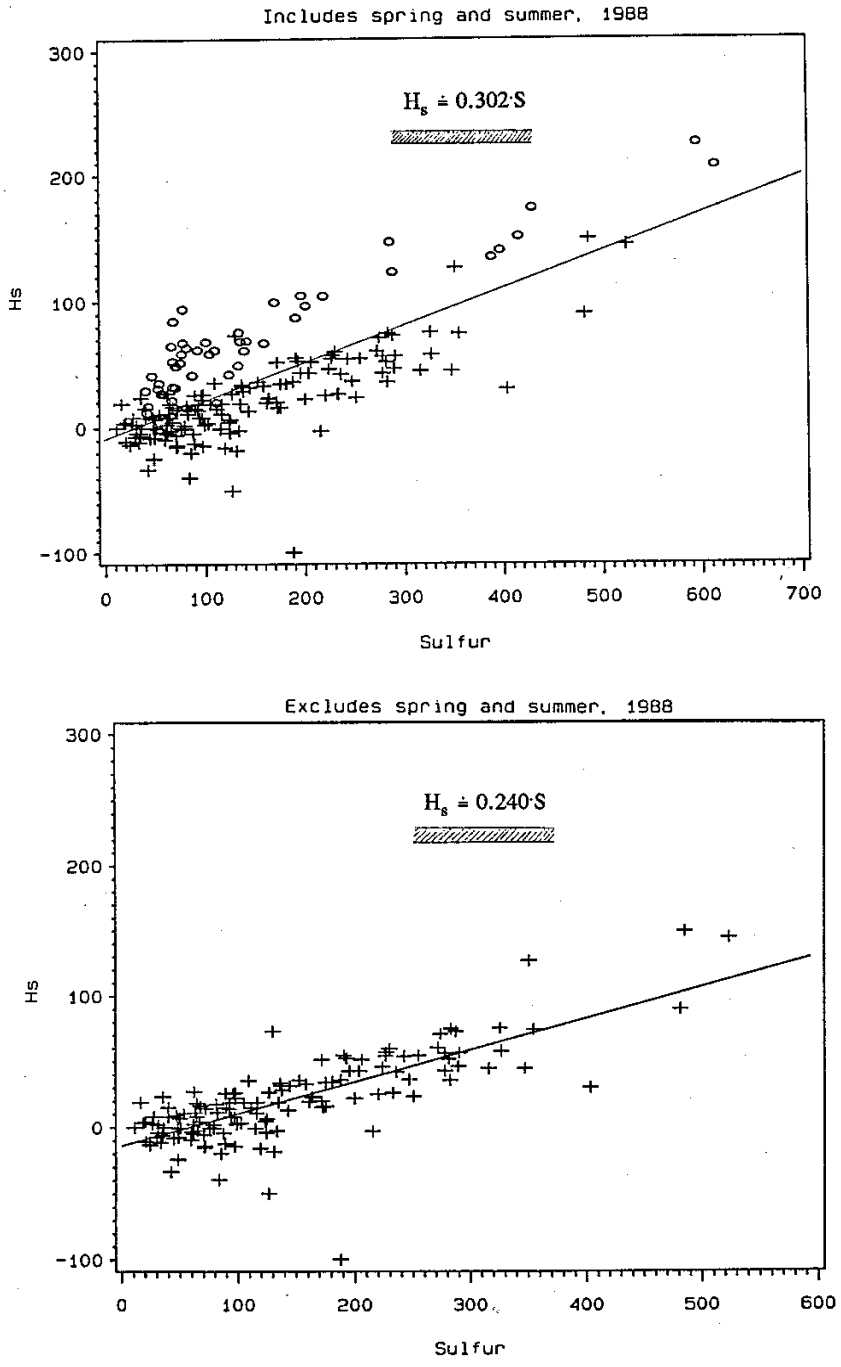

Figure 4.3 Plots of H_s vs. S for Denali. Upper plot includes spring and summer, 1988 (circles), which cause the site to appear overneutralized.

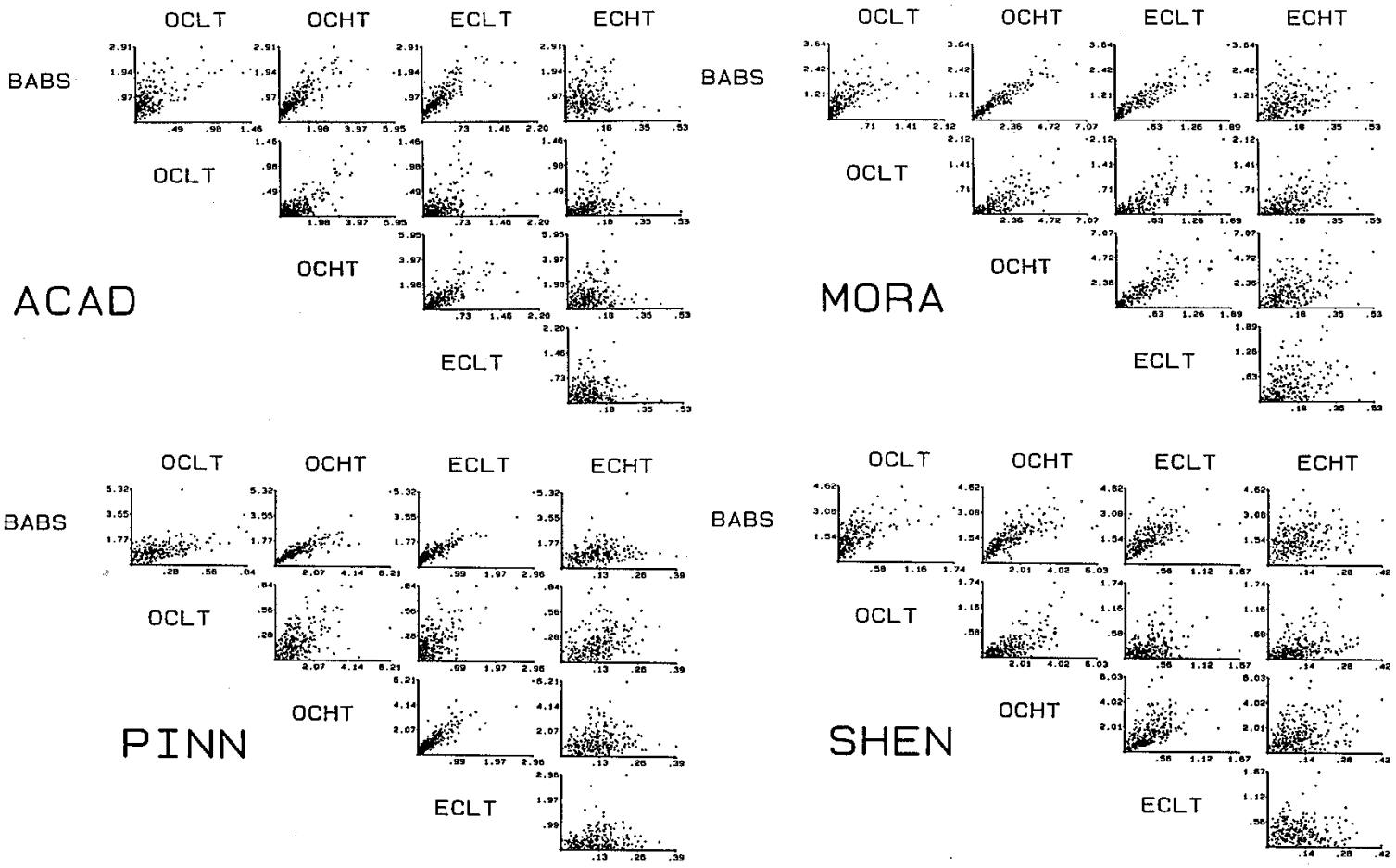

Figure 4.4a Scatter plots of b_{abs} and carbons (OCLT, OCHT, ECLT, ECHT), showing correlation of OCHT and ECLT with b_{abs} and each other, and lack of correlation of ECHT with other species. Units of b_{abs} are 10^{-5}/m; of carbons, $\mu g/m^3$.

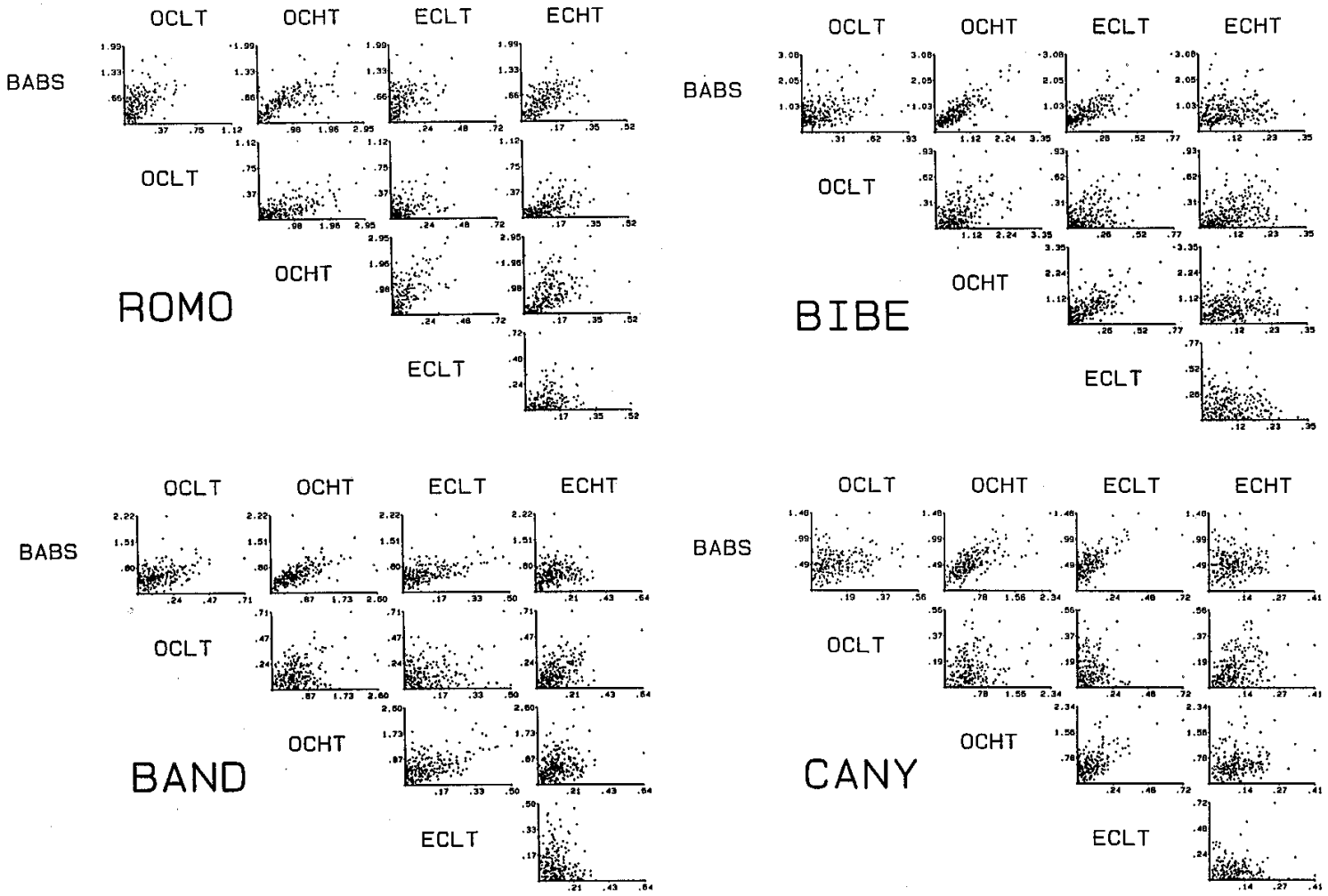

Figure 4.4b. Scatter plots of b_{abs} and carbon species, showing lesser correlation between OCHT and ECLT, and similarity of b_{abs} vs. ECLT and OCHT vs. ECLT plots. Units of b_{abs} are 10^{-5}/m; of carbons, $\mu g/m^3$.

The assignment of approximately half of the light-absorbing carbon to the OCHT at sites such as those represented in Figure 4.4b would reduce the observed absorption efficiency of the carbon approximately from 20 m^2/g to the widely-accepted value of 10 m^2/g. Since the light-absorbing carbon appears to be principally divided between OCHT and ECLT, and the underlying ratio of these two species is about 4 to 1, it follows that approximately 25% of the TOR-reported OCHT at these sites may be light-absorbing carbon.

These results are best explained as due to systematic error in the TOR carbon analysis. (The alternatives, of systematic error in b_{abs} or in the presumed absorption efficiency of carbon, would not explain the correlations noted above.) Consideration of the probable nature of the TOR error is necessary here, in order to clarify the current state of carbon analysis, and to contrast the measurements provided by carbon analysis with those demanded by visibility research. Previous analyses have assumed that the division of carbon into organic and elemental forms coincides with the division between light-absorbing and non-light-absorbing carbon. Considering this, the error in TOR indicated by the present analysis is appropriately explained as the misidentification of substantial elemental carbon as organic carbon. Such an error in the demarcation between organic and elemental carbon, the so-called "OC/EC split", might appear to be the most likely explanation for the present results. However, the possibility of such an error is particularly addressed in comparisons of various carbon analysis methods.

TOR has been directly compared with other carbon analysis methods (Chow et al., 1992), including: Thermal/Optical Transmittance (TOT, which differs from TOR only in using transmittance monitoring instead of reflectance to correct for the charring); Thermal Manganese Oxidation (TMO, in which the oxidizing agent, MnO_2, is present and in contact with the sample throughout the analysis); carbon spiking experiments (in which precisely controlled amounts of organic or elemental carbon are injected onto a clean filter using a microsyringe); and optical absorption. TOT, and hence indirectly TOR, has also been compared with photoacoustic spectroscopy (Turpin et al., 1990), which tracks the light absorption of an ambient aerosol sample. (In this analysis, the sample's absorption of a modulated laser beam produces heating effects in the sample which can be monitored as an acoustic signal.)

It should be noted that as far as the thermal carbon analysis methods (TOR, TOT, TMO, etc.) are concerned, there is no common definition of organic or elemental carbon (Chow et al., ibid.). Each of the methods divides the analyzed carbon into segments which are defined by 1) temperature, 2) rate of temperature increase, 3) composition of atmosphere surrounding the sample, and 4) method of optical correction for the observed charring. All of the carbon analysis methods, including photoacoustic spectroscopy, divide the carbon into organic and elemental forms, and identify the light-absorbing carbon as primarily elemental carbon. They tend to agree well in analyses of standard compounds of elemental or organic carbon, and of diesel fuel emissions, but not so well in analyses of various natural, and apparently more complex, woodsmoke sources of carbon.

The results of the comparisons of TOR with other carbon analysis methods indicate that TOR compares fairly well, and is therefore as good as any other method. However, where the agreement is not so good, TOR is considered more likely to overestimate the elemental carbon than to underestimate it, with respect to some other analysis methods (Chow et al., ibid.). Furthermore, evidence for elemental carbon misidentified as organic is expected to be seen during the TOR analysis in either the optical reflectance monitoring or in observed coloration of the evolved material, and it is generally not. Therefore, a systematic error in the OC/EC split by TOR, in the context of other carbon analysis methods and their assumptions regarding carbon, is not particularly indicated.

However, if the light-absorbing carbon in OCHT is in fact not elemental but organic, the situation is changed. TOR is then not necessarily in error at all (as its comparisons with other methods indicate); its reported measurements are simply not directly interpretable as light-absorbing and non-light-absorbing carbon. If the light-absorbing portion of OCHT were identified primarily with the TOR pyrolyzed carbon (see Figure 2.2 and the related discussion in Section 2.1.1), every difficulty might be overcome. This is the one portion of evolved carbon which, if it were light-absorbing in the original state, would nevertheless not be observed as such in the TOR analysis. (It is interpreted as being light-absorbing only as a result of pyrolysis during the TOR analysis.) It is also the portion that emerges as most problematical in the comparisons of various carbon analysis methods, and the portion present in woodsmokes but absent from diesel fuel emissions (Chow et al., ibid.). Therefore, the TOR pyrolyzed carbon is the most probable candidate for additional light-absorbing carbon. The pyrolyzed carbon area indicated in Figure 2.2 (which is an analysis performed on a sample from Yellowstone) has been evaluated as 25% of the total carbon area denoted as OCHT in that figure. This agrees remarkably well with the quantitative conclusion presented above concerning the light-absorbing carbon which may be contained in OCHT at many rural western sites.

The extinction reconstructions calculated in Chapter 6 follow the traditional approach and assume that all absorption is due to LAC=ECLT+ECHT, with an efficiency of 10 m^2/g. However, the above discussion suggests that a better estimate for light absorption is b_{abs} itself, and that a better estimate for LAC is the use of $b_{abs}/(10\ m^2/g)$.

4.3 Fine Mass

Another validation check is performed by comparing the measured fine mass to a reconstructed fine mass composed of sulfates, organics, light-absorbing carbon and soil, according to the formula:

$$FM = SO_4 + OMC + LAC + SOIL \tag{4.6}$$

where the variables on the right side of the equation are derived from reported IMPROVE variables, according to the following equations (explained in Chapter 3):

$$SO_4 = 4.125[S], OMC = 1.4[OCLT + OCHT], LAC = [ECLT + ECHT] \quad (4.7)$$

and

$$SOIL = 2.20[Al] + 2.49[Si] + 1.63[Ca] + 2.42[Fe] + 1.99[Ti] \quad (4.8)$$

The measurements of S, OC and LAC by IMPROVE have been discussed previously. The soil elements are measured in Channel A by PIXE analysis of the Teflon filter. The reconstructed fine mass thus involves Channels A and C, and it is compared with the Channel A fine mass measurement. Nitrates are not included in the reconstructed fine mass used in this comparison with the Channel A fine mass measurement, because they are volatile and not efficiently collected on Teflon. Also, nitrates (as properly measured off Channel B) comprise less than 15% of the total reconstructed fine mass at all sites outside of California (see Chapter 5).

Figure 4.5 shows typical scatter plots comparing measured and reconstructed fine mass. Scatter plots for all sites are given in Appendix D. The difference between the measured and reconstructed fine mass is denoted as unexplained mass. Measured mass is generally larger than reconstructed, and the unexplained mass is positive. The unexplained mass is thought to be residual water on the filter at the time the filter is weighed. It is greatest at sites with higher relative humidities. In the fine mass reconstruction, LAC could be replaced by $b_{abs}/(10\ m^2/g)$. Similarly, OMC could be replaced by OMH, particularly where the organic mass is small and the hydrogen measurement would be more accurate than the carbon. Time lines of the ratio of measured fine mass to reconstructed are provided in Appendix E for all sites, and Figure 4.6 gives typical examples.

It was discovered that the ratio of measured to reconstructed fine mass exhibits anomalously large values and swings in value at many sites in the middle to latter part of 1990. Data analysis was performed at the National Park Service, Colorado State University, including organics-by-carbon vs. organics-by-hydrogen plots and H_s vs. S studies of acidity. This analysis suggested a possible excess hydrogen problem, which might be due to water or an organic artifact. A typical example of the observed effect of the artifact upon data plots is shown in Figure 4.7 for the Bandelier site.

An extensive study of the problem at all sites was performed by University of California (UCD). From March 1988 to September 1990, they reported, there was excellent agreement between the OMH measured off the Channel A Teflon filters and the OMC measured off the Channel C quartz filters (Figure 4.2). However, from September 1990, the Teflon measurements showed occasional but large positive offsets relative to the quartz measurements (Figure 4.8). During this latter period, the sulfur concentrations on Teflon maintained excellent agreement with the sulfate from corresponding nylon filters (Figure 4.9). The other IMPROVE data indicated the artifact was strictly organic and affected only the hydrogen (thus OMH) and fine mass measurements on the Channel A Teflon filter. Extensive tests, at Desert Research Institute and UCD, of the Channel C TOR organic carbon analysis of the quartz filter, supported the OMC

measurement and indicated the problem was not analytical.

The problem began with a shipment of Teflon filters used between September 1990 and November 1991. An earlier batch, in April 1990, also had a problem--a bowing of the filter due to the support ring--and had been returned to the manufacturer. This batch had serious quality control problems, such as occasional small holes, debris, and shiny flecks (the last evidently caused by improper maintenance of the die). The organic artifact was difficult to define because it was not readily observable on clean filters, but became evident after interaction with the air. It appeared on a relatively small fraction of filters, and it appears to have been associated with the manufacturing of the ringed filter, although UCD could not rule out the possibility of problems with the Teflon filter material itself.

Scanning electron microscope analysis of filters with the identified artifact showed the artifact to be a relatively flat material that blocks out all view of the Teflon substrate in the region of the artifact. Some of the artifact was seen on the back side of the filter.

One result of this discovered artifact was a decision to discontinue using recycled polyolephin in the filter support rings. The filter manufacturer's quality control procedures have been improved, and a new batch of Teflon material was produced. A prototype batch was scheduled to arrive in April 1992, and the first filters from the production run of this material were due to be received in May 1992.

Because of this artifact in the third year of data, only the data for the first two years were used in those areas of study affected by the artifact, including estimations of acidity and the reconstruction of fine mass by principal aerosol species.

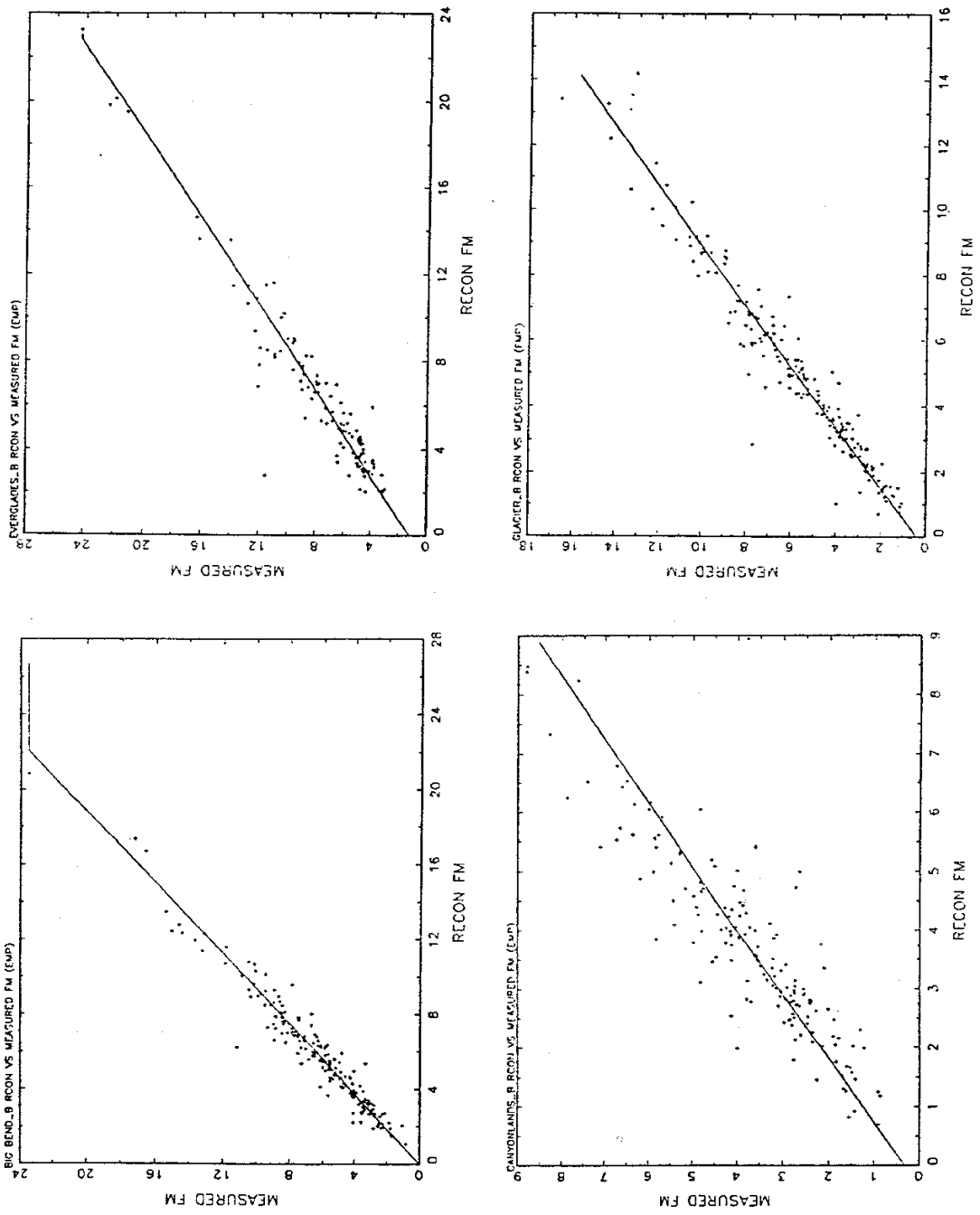

Figure 4.5 Comparisons of measured and reconstructed fine mass.

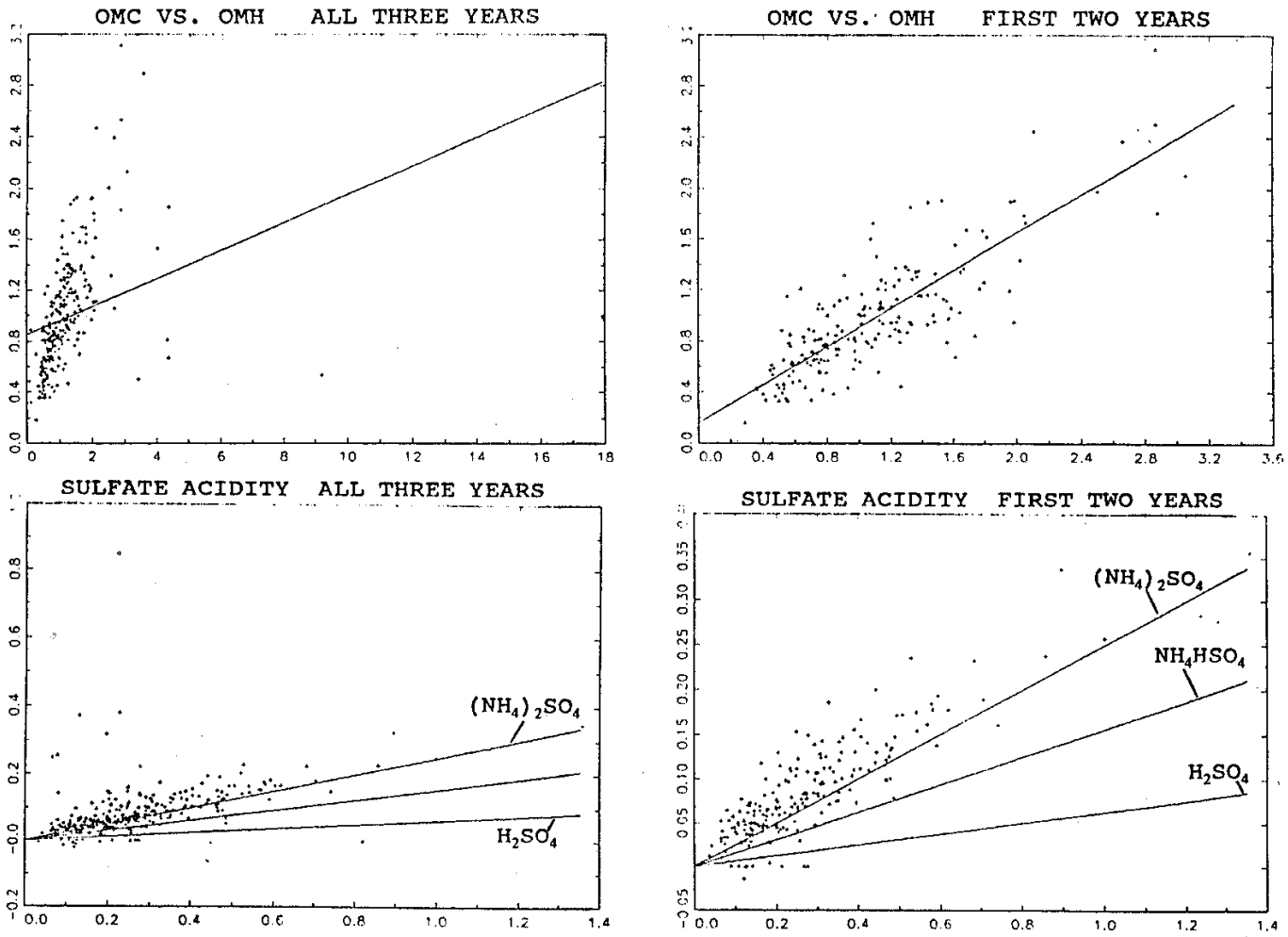

Figure 4.7 Typical effects of the artifact in the third year. The upper pair of plots are OMC vs. OMH; the lower, sulfate acidity. Left-hand plots include data from the third year; right-hand plots do not. Deviations are few, and indicate elevated hydrogen.

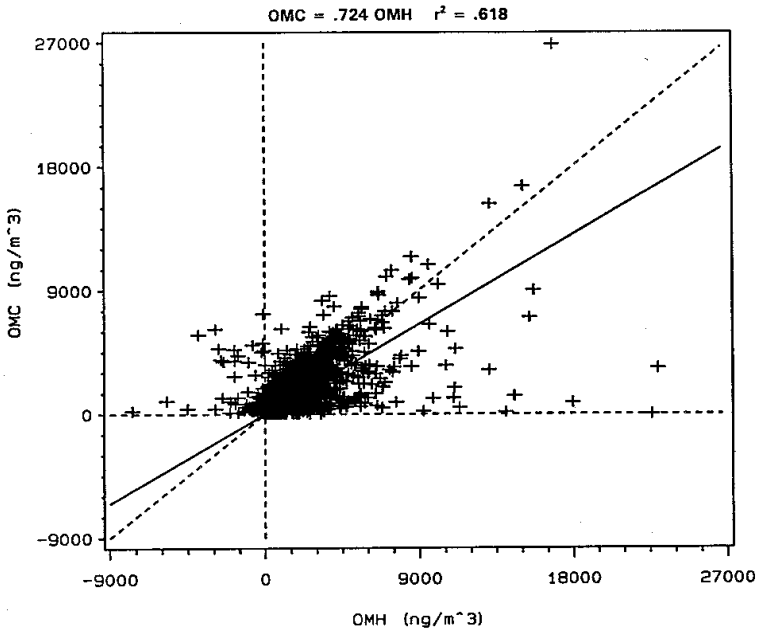

Figure 4.8 OMC versus OMH for the period of the Teflon artifact.

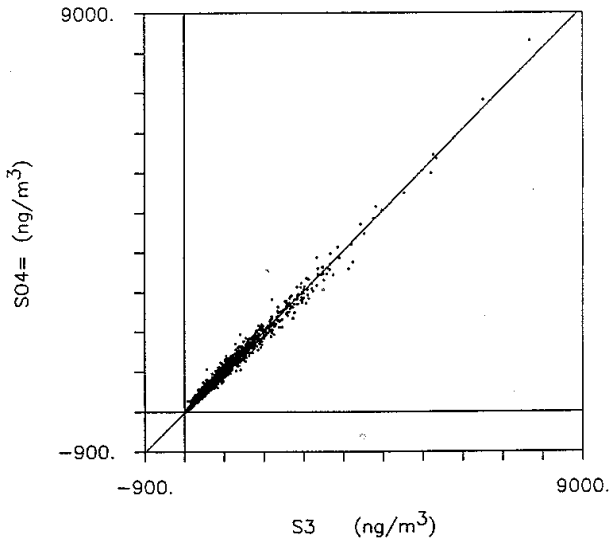

Figure 4.9 SO_4 versus 3·S for the period of the Teflon artifact.